24. INVESTIGATING THE INFLUENCE OF ANTHROPOGENIC FORCING AND NATURAL VARIABILITY ON THE 2014 HAWAIIAN HURRICANE SEASON

Hiroyuki Murakami, Gabriel A. Vecchi, Thomas L. Delworth, Karen Paffendorf, Richard Gudgel, Liwei Jia, and Fanrong Zeng

New climate simulations suggest that the extremely active 2014 Hawaiian hurricane season was made substantially more likely by anthropogenic forcing, but that natural variability of El Niño was also partially involved.

Introduction. Three hurricanes approached the Hawaiian Islands during the 2014 hurricane season (Fig. 24.1a), which is the third largest number since 1949 (black bars in Fig. 24.1b). Previous studies suggest that the frequency of tropical cyclones (TCs) around Hawaii will increase under global warming (Li et al. 2010; Murakami et al. 2013). The projected increase is primarily associated with a northwestward shifting of TC tracks in the open ocean southeast of the islands, where climate models robustly predict greater warming than the other open oceans. Natural variability, such as that associated with the El Niño–Southern Oscillation (ENSO), also has a significant influence on TC activity near Hawaii (Chu and Wang 1997; Jin et al. 2014). In fact, moderate El Niño conditions were observed during the 2014 hurricane season that might have been favorable for TC activity near Hawaii. In this study, we use a suite of climate experiments to explore whether the unusually large number of Hawaiian TCs in 2014 was made more likely by anthropogenic forcing or natural variability.

Methodology. We explore a suite of simulations using the Geophysical Fluid Dynamics Laboratory (GFDL) Forecast-oriented Low Ocean Resolution model (FLOR; Vecchi et al. 2014; see Supplementary Material). Simulated TCs were detected using an automated tracking algorithm as proposed by Murakami et al. (2015; see online supplemental material). For the observational dataset, we used "best-track" data obtained from the International Best Track Archive for Climate Stewardship (IBTrACS; Knapp et al. 2010) and the Unisys Corporation website (Unisys 2015) for the period 1949–2014. We focus on TCs with tropical storm strength or stronger. For the observed sea surface temperature (SST), we used the Hadley Center Global Sea Ice and Sea Surface Temperature dataset (HadISST1; Rayner et al. 2003). We define simulated/observed TCs near Hawaii as those TCs propagating within the coastal region of the Hawaiian Islands; that is, the zone extending 500 km from the coastline (see blue domain in Fig. 24.1a). We performed a preliminary investigation of the dependence of distance on the effect of anthropogenic forcing and natural variability on TC frequency near Hawaii, which revealed that the dependence is small qualitatively.

To assess the ability of FLOR to predict the TCs near Hawaii, we first analyzed a retrospective seasonal forecast made using FLOR initialized on 1 July for each year of 1980–2014 (Vecchi et al. 2014; Jia et al. 2015; see online supplemental material). Figure 24.2a shows the time series of TC number predicted by FLOR, which reasonably predicts the interannual variations of observed TC frequency ($r = 0.59$). Moreover, FLOR predicted marked multidecadal variations in the probability of TC occurrence (for example, higher during the period 1980–94 relative to 1995–2014), which is consistent with the observed variability. However, FLOR underestimates TC number in the abnormal years of 1982, 2009, and 2014, although FLOR predicts relatively larger numbers in 2009 and 2014 compared to the mean of the last two decades (1995–2014). The deficiency in predicting the abnormal years indicates that there may be another forcing that is missing in the experimental setting (for example, atmospheric initialization; aerosols). Or

AFFILIATIONS: Murakami, Vecchi, Delworth, Paffendorf, and Jia—NOAA/Geophysical Fluid Dynamics Laboratory, and Atmospheric and Oceanic Sciences Program, Princeton University, Princeton, New Jersey; Gudgel and Zeng—NOAA/Geophysical Fluid Dynamics Laboratory. Princeton, New Jersey

DOI:10.1175/BAMS-D-15-00119.1

A supplement to this article is available online (10.1175/BAMS-D-15-00119.1)

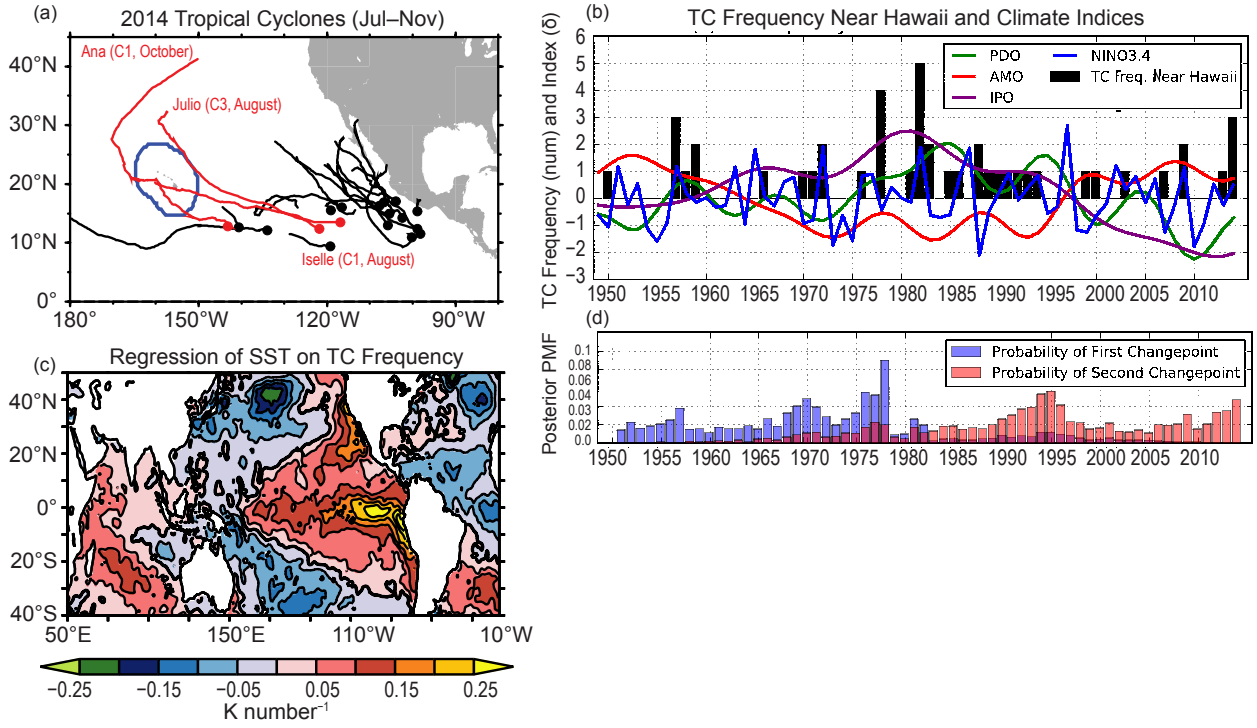

Fig. 24.1. Observed TCs near Hawaii and indices of natural variability. (a) TCs in 2014. Three TCs (red: Iselle, Julio, and Ana) approached the coastal region of Hawaii (blue). Dots denote TC genesis locations. C1 and C3 indicate category 1 and 3 TCs by the Saffir–Simpson hurricane wind scale, respectively. (b) Yearly variability in the number of TCs near Hawaii during the peak season of Jul–Nov for the period 1949–2014 (black bars, number). Colored lines denote climate indices for the PDO (green), AMO (red), IPO (purple), and Niño-3.4 (blue). Units for the indices are one standard deviation. For details of the climate indices and methods used to detect them, see the online supplemental material. (c) Regression of seasonal mean sea surface temperature (SST) onto the number of TCs near Hawaii. Units: K number^{-1}. (d) Results of change-point analysis applied to TC frequency near Hawaii showing the posterior probability mass function (PMF) for the year of the first change point (blue) and second change point (red) under the hypothesis of two change points.

these abnormal events may be unpredictable because of random noise emerging in nature.

Hereafter, we will examine the empirical probability of exceedance for the frequency of TCs near Hawaii during July–November as a function of TC number using the following equation:

$$P(x) = \frac{Number\ of\ years\ with\ TC\ number \geq x}{Total\ number\ of\ years} \qquad (1)$$

where x is the annual number of TCs near Hawaii. For example, *P(3)* represents the probability of occurrence of a year with three or more TCs near Hawaii.

Effect of Anthropogenic Forcing on TCs near Hawaii. Here we form a preliminary estimate of the impact of anthropogenic forcing on Hawaiian TCs, comparing a pair of control climate simulations using FLOR, which were run for 2000-yr (500-yr) intervals by prescribing radiative forcing and land-use conditions representative of the year 1860 (1990) (see online supplemental material). The probability of exceedance for seasonal Hawaiian TC frequency in the 1990 control experiment compares much more reasonably with the observed probability than does the 1860 control experiment (Fig. 24.2b), although the 1990 control experiment still slightly underestimates the observed values. The 1860 control experiment shows substantially reduced probability relative to the 1990 control experiment. The *P(2)* and *P(3)* from the 1990 control experiment are about 5 and 17 times, respectively, larger than those from the 1860 control experiment, or a fraction of attributable risk (FAR; Jaeger et al. 2008) of 80% and 94%, respectively. These experiments suggest that anthropogenic forcing has substantially changed the odds of TC seasons like 2014 near Hawaii relative to natural variability alone.

Effect of Natural Variability on TCs near Hawaii. The black bars in Fig. 24.1b reveal substantial interannual and decadal variations—including a relatively inactive era for Hawaiian TCs for the decade prior to 2014.

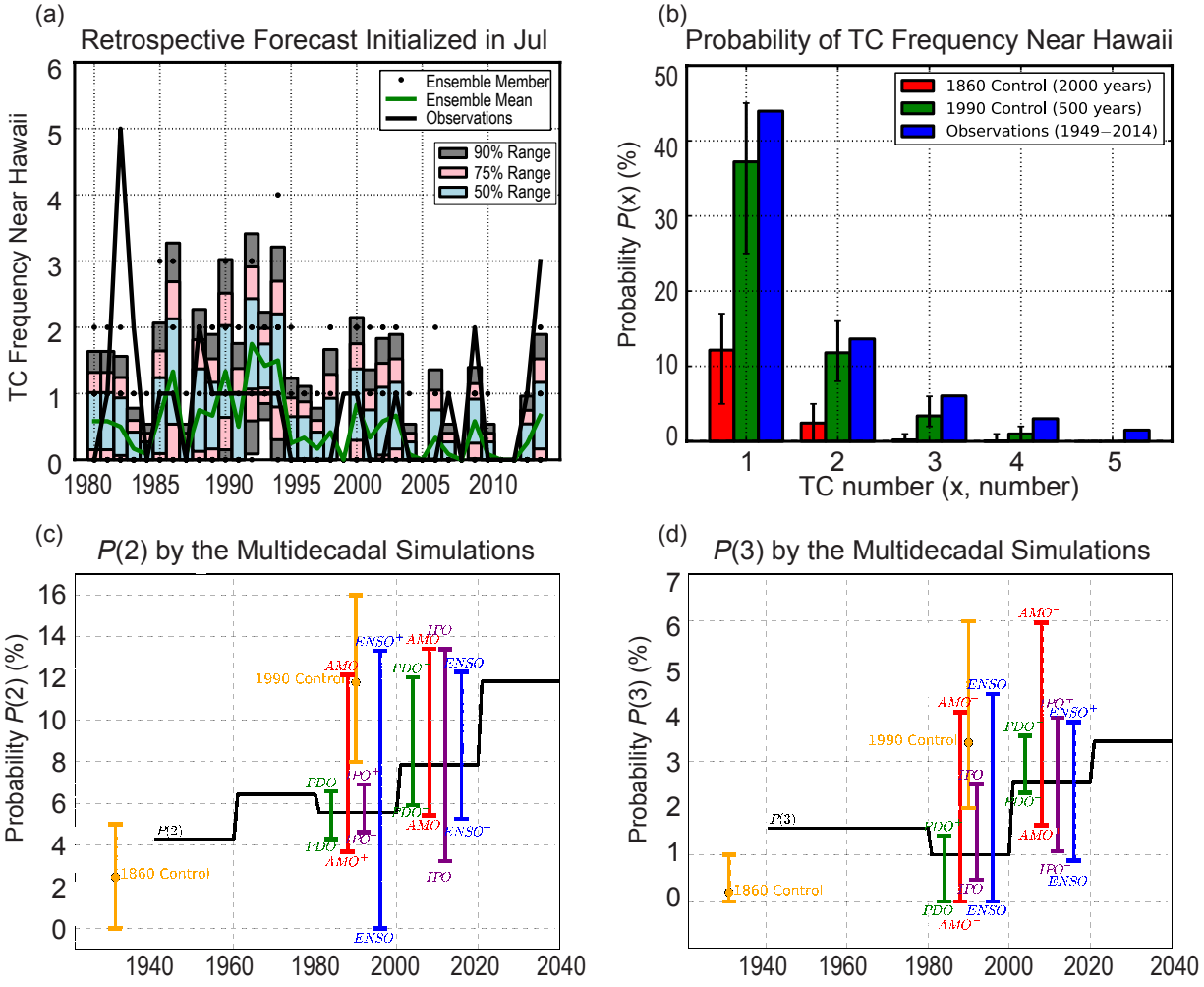

Fig. 24.2. Probability for the frequency of TCs near Hawaii between Jul and Nov simulated by a suite of simulations using FLOR. *P(2)* represents the probability of occurrence of a year with TC number more than or equal to near Hawaii. (a) Retrospective forecasts for TC frequency near Hawaii initialized in Jul. The black line indicates observed TC frequency, green line indicates the mean forecast value, shading indicates the confidence intervals, dots indicate values simulated by one or more ensembles. (b) Results of *P(x)* from the control simulations and observations. Blue bars are probability obtained by observations (1949–2014). Green bars are the results from the 1990 control simulation (500 years), whereas red bars are the results from the 1860 control simulation (2000 years). Error bars in the control simulations denote the range of minimum and maximum values of *P(x)*, computed from each 100-year period. (c) Results of *P*(2) from the multi-decadal simulation. For each 20-year period, *P(2)* (black line) was calculated from 700 samples. Colored bars show the range of conditional *P(2)* induced by natural variability. For example, red bars cover $P(2|AMO_+)$ and $P(2|AMO_-)$, namely, the range of *P(2)* under the conditions between positive AMO and negative AMO phases. Likewise, *P(2)* under the condition of positive and negative phases of PDO (green), ENSO (blue), and IPO (purple) are shown. Orange circles denote results of *P(2)* from the control simulations. The orange error bars show the range of minimum and maximum when *P(2)* is computed for each 100-year period. (d) As (c), but for *P(3)*.

Figure 24.1c shows the seasonal mean SST regressed onto TC frequency near Hawaii, and reveals an El Niño-like spatial pattern. This reflects the tendency for an increase in Hawaiian TC activity during El Niño: the Niño3.4 index (blue line, Supplemental Fig. S24.2) is moderately correlated with TC frequency (Chu and Wang 1997). Moreover, Fig. 24.1b reveals marked multidecadal variations in the TC frequency near Hawaii. There appear to be abrupt shifts in Hawaiian TC frequency in the mid-1970s and 1990s. We applied a change-point analysis developed by Zhao and Chu (2010) to the TC frequency time series, which indicated that the most likely first (second) change point was 1978 (1995) (Fig. 24.1d). The spatial pattern

shown in Fig. 24.1c is also similar to the low-frequency variations of the Pacific Decadal Oscillation (PDO; Mantua et al. 1997; green line, Supplementary Fig. S24.3) or Interdecadal Pacific Oscillation (IPO; Power et al. 1999; Folland et al. 2002; purple line, Supplementary Fig. S24.4). Both indices changed sign around 1997 (Fig. 24.1b), which may contribute to the multidecadal variations in TC frequency (Wang et al. 2010). Moreover, Fig. 24.1c shows marked negative SSTs in the tropical Atlantic, indicating reduced TC frequency near Hawaii when the tropical Atlantic is warmer. A recent study by Kucharski et al. (2011) reported that the Atlantic warming in the late twentieth century could have led to a reduction in Pacific warming via the Walker circulation. The Atlantic multidecadal oscillation (AMO; Delworth and Mann 2000; red line, Supplementary Fig. S24.5) index also changed sign around 1997 (Fig. 24.1b), and this could have caused the abrupt shift in TC frequency.

To elucidate the potential influence of the natural variability outlined above on TC frequency near Hawaii, we conducted 35-member ensemble multidecadal simulations (see online supplemental material) from 1941 to 2040. For each 20-year period from 1941, 700 (20×35) samples were available to calculate *P(x)*. In contrast to the seasonal forecasts, because the simulated internal variability is out of phase among the ensemble members (even with the observations), we can estimate the conditional probability of *P(x)* under any phase of natural variability. In other words, we can estimate potential probability under any phase of natural variability in a specific range of decades. Here, we define a simulated/observed positive (or negative) phase of ENSO, PDO, IPO, and AMO as these indices exceeding one standard deviation and estimate the amplitude of *P(x)* between the two phases. For details of the climate indices and methods used to detect them, see the online supplemental material.

Figures 24.2c and d summarize the results for *P(2)* and *P(3)*. Similar results were obtained for *P(1)* (figure not shown). The black lines show *P(2)* and *P(3)* , and reveal a gradual increase from 1940 to 2040, indicating that global warming generates more TCs near Hawaii, which is consistent with the control simulations. The colored bars denote the range of conditional probability induced by natural variability, revealing that natural variability has considerable potential to influence the probability of TC frequency. The amplitude of the bars is similar to the amplitude of the global warming effect (that is, the difference in orange circles in Figs. 24.2c and d), implying that internal variations could act to either temporarily mask or substantially amplify the impact of anthropogenic forcing on the number of TCs near Hawaii.

Discussions and Conclusions. As shown in Fig. 24.1b, the observed TC frequency was greater during the period 1980–94 than 1995–2014. Moreover, the observations show positive PDO and IPO indices, as well as a negative AMO index between 1980 and 1994, whereas these indices reversed sign between 1995 and 2014. From Figs. 24.2c and d, it is possible that the earlier decades (1981–2000) could have had a higher probability of TC occurrence than more recent decades (2001–20), provided that the PDO, IPO, and AMO indices were more favorable for TC activity during the previous decades. Therefore, it can be concluded that the observed multidecadal difference between 1980–94 and 1995–2014 was mainly caused by natural variability. However, the extremely large number of TCs during the 2014 hurricane season occurred despite the unfavorable IPO (–2.0), AMO (+0.7), and PDO (–0.7), and moderate El Niño (+0.5). The FLOR suggests that historical global warming could have contributed to a substantial increase in probability of active Hawaiian TC seasons. The evidence for this can be shown by the composites of the years in which the phase of natural variability is similar to 2014 case in the control experiments. We found that *P(1)* from the 1990 control experiment under the condition of negative IPO, positive AMO, negative PDO, and moderate El Niño is about 3.4 times larger than that from the 1860 control experiment (FAR = 71%). Therefore, it is possible that global warming increased the odds of the extremely large number of Hawaiian TCs in 2014, in combination with the moderately favorable condition of El Niño. The ensemble experiments with FLOR indicate a continued increasing probability of active seasons around Hawaii over the next few decades [consistent with Murakami et al. (2013)]—although there will be substantial modulation on interannual and decadal timescales from internal variability.

ACKNOWLEDGMENT. This report was prepared by Hiroyuki Murakami under award NA14OAR4830101 from the National Oceanic and Atmospheric Administration, U.S. Department of Commerce. The statements, findings, conclusions, and recommendations are those of the authors and do not necessarily reflect the views of the National

Oceanic and Atmospheric Administration, or the U.S. Department of Commerce.

REFERENCES

Chu, P.-S., and J. Wang, 1997: Tropical cyclone occurrences in the vicinity of Hawaii: Are the difference between El Niño and non-El Niño years significant? *J. Climate*, **10**, 2683–2689.

Delworth, T. L., and M. E. Mann, 2000: Observed and simulated multidecadal variability in the Northern Hemisphere. *Climate Dyn.*, **16**, 661–676.

Folland, C. K., J. A. Renwick, M. J. Salinger, and A. B. Mullan, 2002: Relative influences of the Interdecadal Pacific Oscillation and ENSO on the South Pacific Convergence Zone. *Geophys. Res. Lett.*, **29** (13), doi:10.1029/2001GL014201.

Jaeger, C. C., J. Krause, A. Haas, R. Klein, and K. Hasselmann, 2008: A method for computing the fraction of attributable risk related to climate damages. *Risk Anal.*, **28**, 815–823.

Jia, L., and Coauthors, 2015: Improved seasonal prediction of temperature and precipitation over land in a high-resolution GFDL climate model. *J. Climate*, **28**, 2044–2062,doi:10.1175/JCLI-D-14-00112.1.

Jin, F.-F., J. Boucharel, and I-I Lin, 2014: Eastern Pacific tropical cyclone intensified by El Niño delivery of subsurface ocean heat. *Nature*, **516**, 82–85, doi:10.1038/nature13958.

Knapp, K. R., M. C. Kruk, D. H. Levinson, H. J. Diamond, and C. J. Neuman, 2010: The international best track archive for climate stewardship (IBTrACS): Unifying tropical cyclone best track data. *Bull. Amer. Meteor. Soc.*, **91**, 363–376,doi:10.1175/2009BAMS2755.1.

Kucharski, K., I.-S. Kang, R. Farneti, and L. Feudale, 2011: Tropical Pacific response to 20th century Atlantic warming. *Geophys. Res. Lett.*, **38**, L03702, doi:10.1029/2010GL046248.

Li, T., M. Kwon, M. Zhao, J.-S. Kug, J.-J Luo, and W. Yu, 2010: Global warming shifts Pacific tropical cyclone location. *Geophys. Res. Lett.*, **37**, L21804, doi:10.1029/2010GL045124.

Mantua, N. J., S. R. Hare, Y. Zhang, J. M. Wallace, and R. C. Francis, 1997: A Pacific interdecadal climate oscillation with impacts on salmon production. *Bull. Amer. Meteor. Soc.*, **78**, 1069–1079.

Murakami, H., B. Wang, T. Li, and A. Kitoh, 2013: Projected increase in tropical cyclones near Hawaii. *Nat. Climate Change*, **3**, 749–754, doi:10.1038/nclimate1890.

——, and Coauthors, 2015: Simulation and prediction of category 4 and 5 hurricanes in the high-resolution GFDL HiFLOR coupled climate model. *J. Climate*, doi:10.1175/JCLI-D-15-0216.1, in press.

Power, S., T. Casey, C. Folland, A. Colman, and V. Mehta, 1999: Interdecadal modulation of the impact of ENSO on Australia. *Climate Dyn.*, **15**, 319–324.

Rayner, N. A., D. E. Parker, E. B. Horton, C. K. Folland, L. V. Alexander, and D. P. Rowell, 2003: Global analysis of sea surface temperature, sea ice, and night marine air temperature since the late nineteenth century. *J. Geophys. Res.*, **108**, 4407, doi:10.1029/2002JD002670.

Unisys, 2015: Unisys Weather Hurricane/tropical data. [Available online at http://weather.unisys.com/hurricane/.]

Vecchi, G. A., and Coauthors, 2014: On the seasonal forecasting of regional tropical cyclone activity. *J. Climate*, **27**, 7994–8016, doi:10.1175/JCLI-D-14-00158.1.

Wang, B., Y. Yang, Q.-H. Ding, H. Murakami, and F. Huang, 2010: Climate control of the global tropical storm days (1965-2008). *Geophys. Res. Lett.*, **37**, L07704, doi:10.1029/2010GL042487.

Zhao, X., and P.-S. Chu, 2010: Bayesian changepoint analysis for extreme events (typhoons, heavy rainfall, and heat waves): An RJMCMC approach. *J. Climate*, **23**, 1034–1046. doi: 10.1175/2009JCL,I2597.1.